Spectrochimica Acta Part A: Molecular and Biomolecular Spectroscopy 99 (2012) 390–393

Contents lists available at SciVerse ScienceDirect

Spectrochimica Acta Part A: Molecular and Biomolecular Spectroscopy

journal homepage: www.elsevier.com/locate/saa

Optical detection of NADH based on biocatalytic growth of Au–Ag core–shell nanoparticles

Lin Tang [a,b,*], Xiaoxia Lei [a,b], Guangming Zeng [a,b,*], Yuanyuan Liu [a,b], Yanrong Peng [a,b], Mengshi Wu [a,b], Yi Zhang [a,b], Can Liu [a,b], Zhen Li [a,b], Guoli Shen [c]

[a] College of Environmental Science and Engineering, Hunan University, Changsha 410082, PR China
[b] Key Laboratory of Environmental Biology and Pollution Control, Hunan University, Ministry of Education, Changsha 410082, PR China
[c] State Key Laboratory for Chemo/Biosensing and Chemometrics, College of Chemistry and Chemical Engineering, Hunan University, Changsha 410082, PR China

HIGHLIGHTS

- We developed an optical NADH sensor by biocatalytic growth of Au–Ag nanoparticles.
- Au seeds-catalyzed NADH-mediated reduction of Ag^+ enables particle growth on chip.
- SEM of sensor morphology before and after reaction revealed a diameter increase.
- Absorption peak of growing particles at 415 nm increases with NADH concentration.
- It was precise, fast, good in storage stability and anti-interference ability.

GRAPHICAL ABSTRACT

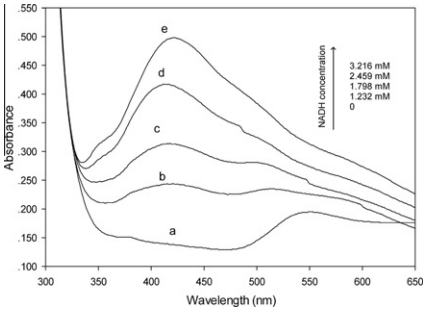

ARTICLE INFO

Article history:
Received 17 April 2012
Received in revised form 26 August 2012
Accepted 4 September 2012
Available online 9 September 2012

Keywords:
Biocatalytic growth
Core–shell nanoparticles
NADH
Biosensor

ABSTRACT

We have developed an optical assay for NADH (Dihydronicotinamide adenine dinucleotide) based on the catalytic growth of gold–silver core–shell nanoparticles (Au–Ag–CSNPs). The nanoparticles were immobilized on pretreated glass slide and are shown to catalyze the NADH-mediated reduction of Ag(I) ions in the presence of 1,4-benzoquinone and cetyltrimethyl ammonium ion. This leads to the formation of Au–Ag–CSNPs on the glass. The absorption peak of the Au–Ag–CSNPs at 415 nm increases with the concentration of NADH in the solution used, and this can be measured by UV–vis photometry. High-resolution scanning electron microscopy analysis of the morphology of the surface of the Au–Ag–CSNPs before and after the catalytic reaction revealed a growth of their diameter. Under optimal conditions, NADH can be determined in the concentration range from 0.2 to 3.2 mM, and the detection limit is 15.6 μM. The sensor has good precision and good storage stability, simple in operation, and can be fabricated at low costs, which made it suitable for the determination of NADH in complex biological systems and in related degradation processes of contaminants.

Introduction

Nanomaterials have attracted widespread attention since the 1990s because of their specific features that differ from bulk materials. The application of nanomaterials to the design of chemical sensors is nowadays one of the most active research fields because of their high activity, good selectivity, tremendous specific surface and small size [1,2]. Thus, immobilized nanoparticles have tremendous potential in a variety of bioanalytical detection schemes [3], and among the various nanomaterials, metal nanoparticles are of particular interests, and have attracted significant attention in the fields of biosensing [4–6]. There are many

* Corresponding authors at: College of Environmental Science and Engineering, Hunan University, Changsha 410082, PR China. Tel./fax: +86 731 88822778.
E-mail addresses: tanglin@hnu.edu.cn (L. Tang), zgming@hnu.edu.cn (G. Zeng).

1386-1425/$ - see front matter © 2012 Elsevier B.V. All rights reserved.
http://dx.doi.org/10.1016/j.saa.2012.09.011

detection methods developed based on their fascinating electronic and optical properties, such as electro generated chemiluminescence for DNA detection [7], fluorescence method for protein assays [8], and electrochemical method for glucose sensing [9].

The special optical properties of nanoparticles showed immense application value which aroused the strong research interests of researchers in biological component analysis field. Recent researches suggest that Au nanoparticles could grow under the catalytic condition of redox active substances with increasing particle size and quantity, which could be quantitative analyzed through UV–vis spectroscopy [10,11]. Baron et al. detected neurotransmitters and tyrosinase activity by noradrenaline-induced growth of Au nanoparticles [12]. Willner et al. developed optical sensors for different substrates by enzyme-mediated growth of metallic nanoparticles [13]. Xiao et al. reported the catalyzed growth of gold nanoparticles in the presence of NAD(P)H cofactors [14]. Core–shell nanoparticles are of considerable interest due to its good performance, and the functional core–shell nanoparticle was widely used in all kinds of biological sensors, such as in electrochemical [15–18], optical [19–21] and piezoelectric biological sensors [22,23]. Optical biosensor selectively identifies molecular information, and that leads to optical change and converts to an electrical signal output. So it has many characteristics, such as, high sensitivity, no reference sensor need, and the light signal transmission is not interfered by external electromagnetic. In addition, it can use for real-time monitoring of biological metabolites [24].

NADH is an important coenzyme involved in metabolic processes, widely existing in every cell of living organisms [25]. It serves as a hydrogen and electron carrier in thousands of metabolism reaction, and alternates between the oxidized state NAD^+ and the reduced state NADH for the production of ATP [26]. More than 300 enzymes are found to be NADH-dependent dehydrogenases, maintaining the cellular growth, differentiation, and energy metabolism [27–29]. At present, the electrochemical method is one of the most frequently used methods for the detection of NADH. For instance, Cui et al. and Gao et al. detected NADH using a glassy carbon electrode [30,31]. Besides, in optical analysis, NADH has distinctive UV absorbance band centered at 340 nm and results in fluorescent signal with an emission maximum of 470 nm. The optical properties are always used in detection of NADH level and enzyme assays for dehydrogenases and reductases with NAD(H) as the coenzyme [14,32]. But many biological molecules can absorb excessive energy in ultraviolet band, which causes light damage, to a greater extent than in visible area or infrared area. And, because the NADH produced by microbes is very low, its absorption spectrum and fluorescence spectrum signals are very weak. Therefore, the methods based on directly measuring its optical effects are not ideal. Although High Performance Liquid Chromatography (HPLC) detection of NADH exhibits good result, it requires expensive equipment costs, professional personnel, and cannot carry out online detection. For this reason, developing an optical detection technology of NADH with good detection effect, simple operation, low cost, and fast speed is an important research topic.

The main purpose of this work was to develop a kind of optical assay to detect NADH concentration. Using the Au nanoparticles fixed on the surface of glass chips as crystal seeds, the existence of NADH aroused the deposition of Ag on the surface of Au nanoparticles and catalytic growth of Au/Ag core–shell nanoparticles. The concentration of NADH was determined by calculating the peak absorbance changes of core–shell nanoparticles in absorption spectrum. After optimizing experimental conditions, this assay could be used in rapid determination of NADH with the advantages of low cost, simple operation and strong anti-interference ability. Meanwhile it provided a faster and more convenient technology to analyze activities of dehydrogenases taking NADH as coenzyme.

Experimental

Reagents

Dihydronicotinamide adenine dinucleotide (NADH), cetyltrimethylamonium chloride (CTAC), HAuCl4, *p*-benzoquinone and glutaraldehyde were of analytical grade and obtained from Sangon Biotech (Shanghai) Co., Ltd (Shanghai, China, http://www.sangon.com/). Au nanoparticles (10 nm in diameter) were from Sino-America Biotechnology Co., Ltd (Beijing, China, http://www.sabc.com.cn/). 3-Aminopropyltrimethoxysilane (APTMS) of analytical grade was obtained from Sinopharm Chemical Reagent Beijing Co., Ltd (Beijing, China, http://www.crc-bj.com/). All the other chemicals were of analytical grade, and all solutions were prepared in deionized water of 18 MΩ purified from a Milli-Q purification system. NADH and *p*-benzoquinone solutions of 0.1 M were daily prepared.

Apparatus

Spectral measurements were performed on UV-2550 UV–vis spectrophotometer (Shimadzu, Japan). The optical path of quartz cell was 1 cm. All the work was done at room temperature (25 °C) unless otherwise mentioned. Scanning electron micrographs (SEM) of the membranes were obtained with a Sirion 200 field emission scanning electron microscope (FEI, Holland). A JEOL JSC-1600 automatic ion sputtering platinum (Japan) was used to spray Pt on the surface of sensor to enhance conductivity.

Preparation of nano-sensor chip

The ordinary slides were made into 30 mm long, 9 mm wide and 1 mm thick, followed by soaking in Pirahna solution (mixture of H_2SO_4, 98% and H_2O_2, 30% with the volume ratio of 4:1) at 60 °C for 20 min. After washing, the slides were soaked in the mixed solution made up of H_2O_2, NH_3 and H_2O (the volume ratio is 1:1:2) at 70 °C for 20 min. They were rinsed with plenty of water and carbinol (chromatographically pure) to remove physical adsorption, and stored in carbinol solution at 4 °C. The slides were put into the mixture of APTMS and carbinol with the volume ratio of 1:1.5 to soak at 35 °C for 18 h, then rinsed with methanol to remove the weak adsorption, and dried in the air. Twenty-five microliters of Au nanoparticles solution with diameter of 10 nm and concentration of 1×10^{-4} M was dropped on the slide and dried in the air at room temperature for 2 h. Then the slides were rinsed with water and stored in water at 4 °C.

Concentration determination of NADH

Twenty-five milliliter ultra-pure water was injected into reference cell and test cell respectively, and then the sensor chip without deposited Ag into test cell was examined by spectral scanning. 0.003 M CTAC, 0.0015 M $AgNO_3$, 0.0015 M *p*-benzoquinone and NADH solutions were added into 3 mL Phosphate Buffered Saline (PBS) (pH 6.64, 1/15 M) in sequence. The sensor chip was quickly immersed in the solutions after mixing and incubated for 8 min at room temperature in dark. Then the sensor chip was taken out, and put into test cell for spectral scanning. According to the peak absorbance value of nanoparticles in absorbance spectrum under the optimal conditions, the concentration of NADH in reaction solution was obtained.

Results and discussions

Characterization of catalytic growth of immobilized Au/Ag NPs

The synthesis procedure of the biosensor and catalytic growth of Au/Ag nanoparticles by NADH (manufacturing process of biosensor and the catalytic growth process of Au/Ag nanoparticles at the condition of catalysis of NADH) was studied clearly (Supplementary material Figure S1). NADH could directly reduce *p*-benzoquinone (Q) to hydroquinone (QH_2), and under the action of hydroquinone (QH_2), Ag^+ was reduced to Ag on the surface of Au nanoparticles. And then core–shell Au/Ag nanoparticles were formed. Reaction equations are as follows:

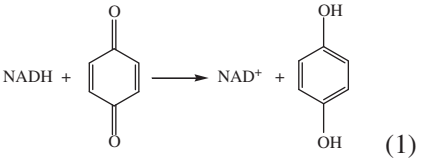

(1) (1)

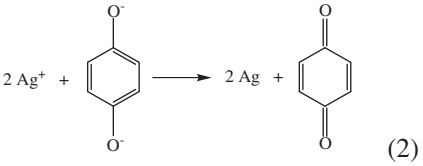

(2) (2)

Twenty-five milliliter ultra-pure water was injected into reference cell and test cell of UV–vis spectrophotometer, respectively, and the sensor chip with deposited Ag was immersed in the test cell for spectral scanning. Au nanoparticles had an absorption peak when wavelength was around 560 nm, and core–shell Au/Ag nanoparticles would form a new absorption peak around 415 nm. Moreover, the new peak increased with the concentrations growth of NADH in the reaction solution. When reaction solution was 3 mL PBS (pH 6.64, 1/15 M) containing CTAC (0.003 M), $AgNO_3$ (0.0015 M) and *p*-benzoquinone (0.0015 M), the sensors could rapidly respond to the concentration variation of NADH. Fig. 1 indicated variations in the absorbance spectra of the Au/Ag nanoparticles growth solution at different concentrations of NADH. As the figure shows, the absorption peak of Au/Ag nanoparticles around 415 nm increased with the concentrations of NADH increasing.

Meanwhile, a JEOL JSC-1600 auto ion sputtering platinum was used to spray Pt on the surface of sensors to enhance conductivity, and the thickness of Pt was about 10 nm. The surfaces of the sensors, both before catalytic growth and after catalytic growth of the Au/Ag nanoparticles were examined by SEM. According to the SEM images (Supplementary material Figure S2), the Au nanoparticles on the sensor's surface before catalytic growth had a size around 10 nm (Figure S2(a)). After catalytic growth cultured in PBS (pH 6.64, 1/15 M) containing CTAC (0.003 M), $AgNO_3$ (0.0015 M), *p*-benzoquinone (0.0015 M) and NADH (6.49×10^{-4} M), the Au/Ag nanoparticles were catalytically enlarged to reach a size around 43 nm (Figure S2(b)). Diameter of Au/Ag nanoparticles obviously increased.

Optimization detecting condition

In the experiments, the sensitivity of sensor is found to be related to the fixed amounts of Au nanoparticles on slides. The more Au nanoparticles were fixed on the slides, the higher the absorption peak of the sensor around 560 nm wavelength is, and the larger the change of response peak was observed for the same concentration of NADH. But the absorption peaks formed by Au/Ag core–shell type nanoparticles at 415 nm wavelength were easy to be obscured while the absorption peaks by Au nanoparticles at 560 nm wavelength were too high. Therefore, the sensor response reached the optimum when the absorption peak value of Au nanoparticles slide was 0.14 at 560 nm wavelength, and at this time, the addition amount of Au nanoparticles solution was 75 μL. In addition, to study the incubation period, it was found that the response peak of the sensor reached maximum after 8 min incubation in reaction solution. So we used 8 min as reaction liquid incubation time to achieve stable response result.

NADH detection

At the optimal detection conditions mentioned above, linear regression method was used to analyze the absorption peak value (I) of Au/Ag nanoparticles in sensor response spectrum and the corresponding NADH concentration (C, 10^{-4} M), shown in Fig. 2. When the NADH concentration was in the range of 2×10^{-4}–3.2×10^{-3} M, the corresponding regression equation is:

$$I = (0.1064 \pm 0.0116) + (0.0119 \pm 0.0006) \times C \quad (3)$$

where the correlation coefficient R^2 is 0.9806, and the detection limit is 1.56×10^{-5} M.

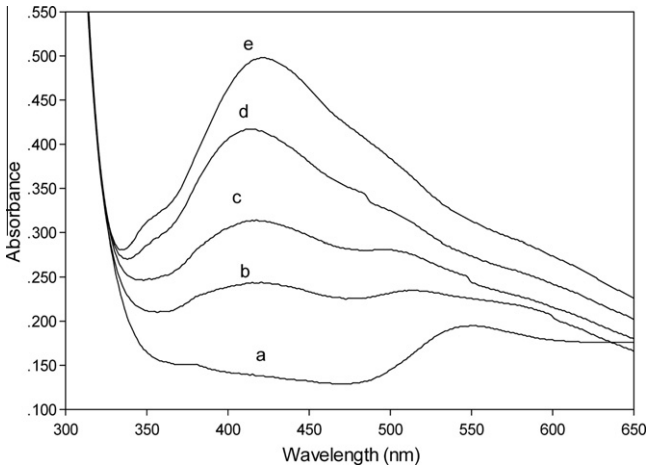

Fig. 1. Variation in the absorbance spectra of the Au/Ag nanoparticles growth solution at different concentrations of NADH: (a) 0, (b) 12.32×10^{-4} M, (c) 17.98×10^{-4} M, (d) 24.59×10^{-4} M and (e) 32.16×10^{-4} M.

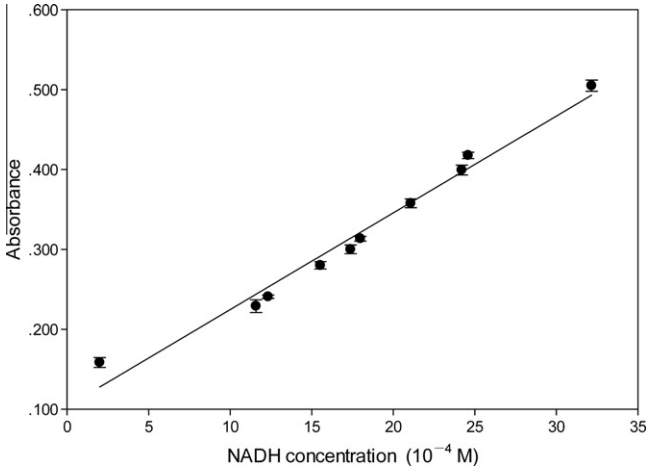

Fig. 2. Linear regression of absorbance vs NADH concentration.

Table 1
Comparison of detection results of NADH concentration by sensor and UV spectrophotometry.

UV spectrophotometry (10^{-4} M)	Biosensor method (10^{-4} M)	Relative error (%)
10.98	9.92	−9.7
17.01	16.62	−2.3
20.77	21.14	1.8
24.89	26.28	5.6

NADH sample test

The detection results by the sensor and UV spectrophotometry for NADH sample solution were compared. Different concentrations of NADH solution were chosen as samples with the wavelength of UV absorption peak of 340 nm. The comparison result is shown in Table 1.

From the above table, it is found that the detection of NADH using this biosensor was accurate and effective.

Conclusions

We describe here, a type of optical nano-detecting chip based on in situ catalytic growth of the immobilized Au/Ag core–shell nanoparticles for the detection of NADH concentration was prepared. Detection chip consisted of the basal layer as incubation reaction seeds and the growth reaction layer of growing nanoparticles. The basal layer was the Au nanoparticles fixed to the slide. In reaction solution containing different concentrations of NADH, Ag^+ was reduced to Ag on the surface of Au nanoparticles, and then Au/Ag core–shell nanoparticles were formed and grown. The concentration of NADH could be calculated by the changes of absorption peak of nanoparticles in spectra. When the NADH concentration was in the range of 2×10^{-4}–3.2×10^{-3} M, this optical assay for NADH detection had good stability. Each of the calibrations was done three times, and the average of the relative standard deviations is 6.1%, which guaranteed the precision of the assay. The detection of NADH at certain concentration was repeated several times in a period of 3 months, and the standard deviations were found to be less than 9%, showing good storage stability. Compared with the existing technology, the assay described here showed the advantages in simple operation, low cost, and could eliminate the interference of ultraviolet-light-absorbing substances existing in biological samples. It could be expected to obtain rapid determination of NADH in complex biological systems and degradation processes of environmental pollutants, and provide a more convenient and efficient way for the activity analysis of oxidoreductases with NADH as coenzyme.

Acknowledgements

The study was financially supported by the Fundamental Research Funds for the Central Universities, Hunan University, the National Natural Science Foundation of China (51222805), and the Program for New Century Excellent Talents in University from the Ministry of Education of China (NCET-11-0129).

Appendix A. Supplementary material

Supplementary material associated with this article can be found, in the online version, at http://dx.doi.org/10.1016/j.saa.2012.09.011.

References

[1] J.J. Shi, Y.F. Zhu, X.R. Zhang, W.R.G. Baeyens, Trends Anal. Chem. 23 (2004) 351–360.
[2] B.I. Ipe, K. Yoosaf, K.G. Thomas, J. Am. Chem. Soc. 128 (2006) 1907–1913.
[3] S.G. Penn, L. Hey, M.J. Natan, Microchim. Acta 165 (2009) 1–22.
[4] L. Shang, H.J. Chen, L. Deng, S.J. Dong, Biosens. Bioelectron. 23 (2008) 1180–1184.
[5] G.M. Zeng, Z. Li, L. Tang, M.S. Wu, X.X. Lei, Y.Y. Liu, C. Liu, Y. Pang, Y. Zhang, Electrochim. Acta 56 (2011) 4775–4782.
[6] Y.Y. Lin, Y.L. Hu, Y.M. Long, J.W. Di, Microchim. Acta 175 (2011) 259–264.
[7] Y. Li, H.L. Qi, J. Yang, C.X. Zhang, Microchim. Acta 164 (2009) 69–76.
[8] B.Y. Hsieh, Y.F. Chang, M.Y. Ng, W.C. Liu, C.H. Lin, H.T. Wu, C. Chou, Anal. Chem. 79 (2007) 3487–3493.
[9] H.Y. Shi, Z.X. Zhang, Y. Wang, Q.Y. Zhu, W.B. Song, Microchim. Acta 173 (2011) 85–94.
[10] M. Zayats, R. Baron, I. Popov, I. Willner, Nano Lett. 5 (2005) 21–25.
[11] Y. Xiao, B. Shlyahovsky, I. Popov, V. Pavlov, I. Willner, Langmuir 21 (2005) 5659–5662.
[12] R. Baron, M. Zayats, I. Willner, Anal. Chem. 77 (2005) 1566–1571.
[13] I. Willner, R. Baron, B. Willner, Adv. Mater. 18 (2006) 1109–1120.
[14] Y. Xiao, V. Pavlov, S. Levine, T. Niazov, G. Markovitch, I. Willner, Angew. Chem. Int. Ed. 43 (2004) 4519–4522.
[15] H. Cai, Y.Q. Wang, P.G. He, Y.Z. Fang, Anal. Chim. Acta 469 (2002) 165–172.
[16] Y. Wang, W.P. Qian, Y. Tan, S.H. Ding, H.Q. Zhang, Talanta 72 (2007) 1134–1140.
[17] J.D. Qiu, H.P. Peng, R.P. Liang, Electrochem. Commun. 9 (2007) 2734–2738.
[18] X.Q. Liu, B.H. Li, X. Wang, C.Y. Li, Microchim. Acta 171 (2010) 399–405.
[19] A. Gopalan, D. Ragupathy, H.T. Kim, K.M. Manesh, K.P. Lee, Spectrochim. Acta A 74 (2009) 678–684.
[20] H.W. Huang, C.C. He, Y.L. Zeng, X.D. Xia, X.Y. Yu, P.G. Yi, Z. Chen, J. Colloid Interface Sci. 322 (2008) 136–142.
[21] D. Enders, S. Rupp, A. Küller, A. Pucci, Surf. Sci. 600 (2006) 305–308.
[22] Y.J. Ding, J. Liu, H. Wang, G.L. Shen, R.Q. Yu, Biomaterials 28 (2007) 2147–2154.
[23] X. Jia, L. Tan, Q.J. Xie, Y.Y. Zhang, S.Z. Yao, Sens. Actuators B 134 (2008) 73–280.
[24] D.G. Bracewell, A. Gill, M. Hoare, P.A. Loweb, C.H. Maule, Biosens. Bioelectron. 13 (1998) 847–853.
[25] L. Tang, G.M. Zeng, G.L. Shen, Y. Zhang, Y.P. Li, C.Z. Fan, C. Liu, C.G. Niu, Anal. Bioanal. Chem. 393 (2009) 1677–1684.
[26] X. Huang, I.H. El-Sayed, X. Yi, M.A. El-Sayed, J. Photochem. Photobiol. B 81 (2005) 76–83.
[27] L. Gorton, E. Dominguez, Rev. Mol. Biotechnol. 82 (2002) 371–392.
[28] L. Tang, G.M. Zeng, H. Wang, G.L. Shen, D.L. Huang, Enzyme Microb. Technol. 36 (2005) 960–966.
[29] L. Tang, G.M. Zeng, G.L. Shen, Y. Zhang, G.H. Huang, J.B. Li, Anal. Chim. Acta 579 (2006) 109–116.
[30] L. Cui, S.Y. Ai, K. Shang, X.M. Meng, C.C. Wang, Microchim. Acta 174 (2011) 31–39.
[31] Q. Gao, M. Sun, P. Peng, H.L. Qi, C.X. Zhang, Microchim. Acta 168 (2010) 299–307.
[32] T. Arakawa, T. Koshida, T. Gessei, K. Miyajima, D. Takahashi, H. Kudo, K. Yano, K. Mitsubayashi, Microchim. Acta 173 (2011) 199–205.